STEM CELLS
TRANSLATIONAL AND CLINICAL RESEARCH

Stem Cell-Derived Therapeutic Myelin Repair Requires 7% Cell Replacement

MARY E. KIEL,[a] CUI P. CHEN,[a] DOROTA SADOWSKI,[a] RANDALL D. MCKINNON[a,b]

[a]Department of Surgery (Neurosurgery), University of Medicine and Dentistry of New Jersey-Robert Wood Johnson Medical School, Piscataway, New Jersey, USA; [b]Department of Molecular Genetics Microbiology, and Member, The Cancer Institute of New Jersey, New Brunswick, New Jersey, USA

Key Words. Cell transplantation • Embryonic stem cells • Glia • Oligodendrocytes • Thresholds

ABSTRACT

Embryonic stem cells (ESCs) hold great potential for therapeutic regeneration and repair in many diseases. However, many challenges remain before this can be translated into effective therapy. A principal and significant limit for outcome evaluations of clinical trials is to define the minimal graft population necessary for functional repair. Here we used a preclinical model for quantitative analysis of stem cell grafts, with wild-type ESC grafted into myelin mutant shiverer hosts, to determine minimum graft levels for therapeutic benefit. Using a timed motor function test we identified three groups, including recipients indistinguishable from nongrafted shiverer controls (time [t] = 20.1 ± 1.1 seconds), mice with marginal improvement (t = 15.7 ± 1 seconds), and mice with substantial phenotype rescue (t = 5.7 ± 0.9 seconds). The motor function rescued chimeras also had a considerably extended life span (T_{50} > 128 days) relative to both shiverer (T_{50} = 108 days) and the nonrescued chimeras. Retrospective genotype analysis identified a strong correlation (r^2 = 0.85) between motor function and ESC-derived chimerism, with > 7% chimerism required for rescue in this murine model of central nervous system myelin pathology. These results establish the minimal levels of engraftment to anticipate therapeutic repair of a cell-autonomous defect by cell transplant therapy. STEM CELLS *2008;26:2229–2236*

Disclosure of potential conflicts of interest is found at the end of this article.

INTRODUCTION

Cell and organ transplant therapy is an established approach in clinical medicine, although the number of conditions that can be addressed using these therapies are relatively limited. The gold standard for cell transplants is in hematopoiesis, where bone marrow stem cells from histocompatible donors can replace those in a cancer patient. These successes have fueled the drive to apply stem cell therapy in a broad range of genetic, acquired, and degenerative diseases. Principle among these are clinically intractable chronic neurodegenerative conditions of the central nervous system [1] including the accumulation of β-amyloid plaques in Alzheimer's disease, the loss of dopaminergic neurons in Parkinson's disease [2], and the loss of myelin-forming oligodendrocytes in multiple sclerosis (MS), the most common neurodegenerative condition of young adults [3].

There are three major hurdles to overcome before stem cell therapy can be a clinical reality for brain repair. First there is a need to identify the disease mechanism in order to define the therapeutic objectives. Although the mechanisms underlying Alzheimer's and Parkinson's disease remain elusive, the immune-mediated loss of myelin in MS is well established, the pathology of the MS lesion is constant [3], and the repair objectives are defined [4]. The second hurdle is the need to identify an appropriate source of cells that can compensate for the cellular deficit. Potential candidates include multipotential neural stem cells [5–8], and in vitro derivatives of pluripotential ESCs [9–11]. ESC technology has been extended to human cells [12], which hold great promise to regenerate any organ system for any disease [1]. However, for both neural stem and ESCs, the current technology is limited to harvesting cells from tissue sources that present significant ethical concerns. Recent advances such as the induction of pluripotent ESCs from autologous fibroblasts [13–15] have the potential to resolve these ethical concerns, as well as address the need for histocompatible grafts. The third hurdle is the need to define how to deliver cells, and how many cells to deliver, to achieve therapeutic benefit. Since the brain and spinal column present tremendous surgical risks, a significant aspect of cell delivery for neural repair is to promote the migration of grafted cells toward target lesions. This may require modifications of the grafted cells, and possibly of the host environment, to encourage cell homing into a lesion [4]. A second aspect is the general question of how many grafted cells are required for functional recovery [16]. In Parkinson's disease, for example, the failure of transplant therapies to date could represent

Author contributions: M.E.K.: conception and design, collection and assembly of data, data analysis and interpretation, manuscript writing; C.P.C.: collection and assembly of data, manuscript writing; D.S.: collection and assembly of data; R.D.M.: conception and design, financial support, data analysis and interpretation, manuscript writing, final approval of manuscript.

Correspondence: Randall D. McKinnon, Ph.D., UMDNJ-Robert Wood Johnson Medical School, 675 Hoes Lane, S-225, Piscataway NJ 08854. Telephone: 732-235-4419; e-mail: mckinnon@umdnj.edu Received March 3, 2008; accepted for publication July 2, 2008; first published online in STEM CELLS *EXPRESS* July 17, 2008. 1066-5099/2008/$30.00/0 doi: 10.1634/stemcells.2008-0218

insufficient numbers of grafted neural precursors [16] rather than an ineffective graft population [2].

The ability of stem cells to generate specific neural cell types has been well established in numerous preclinical transplant models. However, quantitative aspects of graft survival or extent of cell replacement have largely not been addressed to date. In the present study we examine whether the level of cell engraftment correlates with functional outcome. We chose a genetic model of central nervous system (CNS) myelin pathology, the myelin mutant shiverer (*shi*) mice [17]. Shiverer mice lack the myelin basic protein (MBP) gene [18] and produce uncompacted myelin that subsequently degenerates (dysmyelination). This allele affects only CNS myelin, since peripheral myelin generated by Schwann cells is compacted by the P_0 protein [19]. Thus the *shi* phenotype is an effective approximation of CNS-specific demyelination as seen in autoimmune-mediated MS.

Shiverer mice have been used extensively for qualitative outcome evaluation of the myelin-generating potential of graft cell populations, including myelin repair by ESC-derived oligodendrocyte progenitor cells (OPCs) from mice [20, 21] and humans [22, 23], by neural stem cells, and by glial progenitors [24–26]. Shiverer has also been rescued by transgene approaches [27]. Here we use ESC-derived cell therapy and compare functional deficits in chimeric mice with a range of wild-type stem cell-derived grafts. Our results identify limited improvements with as little as 1% engraftment, and substantial improvements in both motor function and longevity in animals with >7% tissue engraftment. This level of cell replenishment thus sets the bar for developing effective ESC-derived stem cell therapeutics. To our knowledge this is the first study to determine the minimal level of engraftment for functional neural cell replacement therapy.

Materials and Methods

Animals

Shiverer (Mbp^{shi}) mice (C3Fe.*SWV-*Mbp^{shi}/J) were obtained from Jackson Laboratory (Bar Harbor, ME, http://www.jax.org). Chimeras were constructed by harvesting day-3.5 MBP^{shi} blastocysts from females of homozygous (*shi/shi*) breeding pairs, injecting $Olig2^{GFP}$ ESCs (n = 14 cells each), then transferring the MBP^{shi}:$Olig2^{GFP}$ chimeric blastocysts into pseudopregnant recipients (Robert Wood Johnson Medical School [RWJMS] Transgenic Core Facility, New Brunswick, NJ). Offspring were tagged (toe) and biopsied (tail) for genotype analysis. All procedures were approved by the institutional animal care and use committee.

Cell Culture

Mouse embryonic fibroblasts (MEFs) were obtained from day-13 embryos of C57Bl/6J mice (Jackson Laboratory) using standard protocols. MEF cells were expanded for up to four passages in Dulbecco's Modified Eagle Media (DMEM, Invitrogen, Carlsbad, CA, http://www.invitrogen.com) supplemented with 10% ESC-tested fetal bovine serum (FBS; Atlanta Biologicals, Lawrenceville, GA, http://www.atlantabio.com) and 1% nonessential amino acids (Invitrogen), using 0.25% trypsin (Invitrogen) to dissociate confluent monolayers of cells from the Falcon 3003 culture plates (Becton Dickinson, Franklin Lakes, NJ, http://www.bd.com). The MEF cells were γ-irradiated (4,000 rad) for mitotic arrest prior to use as ESC feeder layers.

$Olig2^{GFP}$ ESCs, with a green fluorescent protein (GFP) transgene in the Olig2 locus [28], were obtained from American Type Culture Collection, (Rockville, MD, http://www.atcc.org). ESCs were expanded on γ-irradiated MEFs, in 0.1% gelatin-coated plates, in ESC media (DMEM, 15% FBS, 60 μM β-mercaptoethanol, 1% nonessential amino acids) containing 100 units/ml (1.3 ng/ml) recombinant leukemia inhibitory factor (LIF; Chemicon Inc., Temecula, CA, http://www.chemicon.com).

For in vitro gliogenesis [4, 29], ESCs were sequentially exposed to conditions that promote the formation of embryoid bodies (EBs), neuroepithelial stem (NS) cells, ventral neural precursors, and then to conditions that select for the amplification of OPCs. First, ESCs were plated in nonadherent Falcon 1029 bacterial Petri plates (Becton Dickinson) in ESC media without LIF for 4 days to form aggregated EBs. Second, EBs were cultured for 4 days in ESC media containing 500 nM retinoic acid to generate NS cells. Third, the NS cells were dissociated with trypsin and expanded for 2 days as adherent cells with 10 ng/ml basic fibroblast growth factor (FGF2; R&D Systems, Minneapolis, http://www.rndsystems.com) in ITSFn media [20], consisting of DMEM supplemented with 5 μg/ml insulin, 50 μg/ml transferrin, 30 nM sodium selenite, and 5 μg/ml fibronectin (Sigma-Aldrich, St. Louis, http://www.sigmaaldrich.com). Fourth, the NS cells were ventralized by exposure for 2 days the ITSFn/FGF2 media containing 300 ng/ml Sonic hedgehog (Shh; R&D Systems). Fifth, OPCs were expanded by exposure for 5 days in ITSFn containing 40 ng/ml 3,3,5 triiodothyronine (T3) plus 10 ng/ml platelet-derived growth factor (PDGF; R&D Systems). To generate oligodendrocytes (OLs), OPCs were treated for 3 days in ITSFn with T3 and 0.5% FBS.

Immunocytochemistry

Monoclonal antibodies O4 [30] and RmAb [31] were obtained as supernatant fluids from the respective cell lines and polyclonal rabbit anti-MBP was from Chemicon Inc. Cells growing in Lab Tech tissue chamber slides (Nalge Nunc, Rochester, NY, http://www.nuncbrand.com) were fixed (room temperature [temp], 10 minutes) in 4% paraformaldehyde in phosphate-buffered saline (PBS), washed extensively in PBS, then exposed to primary antibodies (room temp, 1 hour) diluted in PBS. The slides were then washed in PBS and exposed (room temp, 1 hour) to secondary antibodies conjugated to fluorescent (Alexa-488, Alexa-544) tags (Molecular Probes, Eugene, OR, http://probes.invitrogen.com). After washing in PBS the slides were mounted under coverslips in mounting media (Vector Laboratories, Burlingame, CA, http://www.vectorlabs.com) containing the nuclear stain 4′,6′-diamidino-2-phenylindole. Tissue sections, or whole mount spinal cords, were fixed overnight at 4°C in 4% paraformaldehyde then processed as above in PBS containing 0.1% Triton X-100. Images were collected in 1-micron z-sections on a Zeiss LSM510 Meta confocal microscope (Carl Zeiss, Jena, Germany, http://www.zeiss.com), and assembled in Adobe Photoshop version 6.0 (Adobe Systems, San Jose, CA, http://www.adobe.com).

Polymerase Chain Reaction

Polymerase chain reaction (PCR) amplification was performed using an Eppendorf Mastercycler gradient thermocycler, and cycle parameters were as follows: 95°C for 2 minutes, 30× (95°C for 30 seconds, 55°C for 1 minute, and 72°C for 2 minutes), 1× 72°C for 10 minutes. The 50-μl reactions contained 1 μg genomic DNA, 0.2 μM PCR primers (Integrated DNA Technologies, Coralville, IA, http://www.idtdna.com) and Taq Polymerase (Invitrogen) with conditions specified by the manufacturer. For transcript analysis, RNA was extracted using TRIzol reagent and copied into cDNA with Moloney murine leukemia virus reverse transcriptase (RT) using conditions specified by the manufacturer (Invitrogen). A portion of the RT-PCR products was examined by agarose gel electrophoresis to determine size relative to a kilobase marker (Invitrogen). For DNA sequence analysis, RT-PCR products were purified by column chromatography (Qiagen, Valencia, CA, http://www1.qiagen.com), then 50 ng DNA was subjected to automated capillary sequencing with 2 pmol of either the forward or reverse PCR primer using an ABI PRISM 3100 Genetic Analyzer (RWJMS DNA Core Facility).

ESC Graft Contribution

Chimerism was determined by real-time quantitative PCR (Q-PCR) using an ABI7900HT and SDS version 2.2 software (Applied Biosystems, Foster City, CA, http://www.appliedbiosystems.com). Cycle conditions were as follows: 50°C for 2 minutes, 95°C for 10

Table 1. Oligonucleotide primers for polymerase chain reaction (PCR) amplification

Gene	NCBI ID	Primers
GAPDH	BC083080	5′-agccaaaagggtcatcatctc
		5′-ctgtggtcatgagtccttcca
MBP (intron 1)	AC158975	5′-gaggccgcacatcagccctgattttgctaag
		5′-gataggactggcctctgctgctt
		5′-ctcaccgtcctgagaccatt
		5′-cactgtctccaggggaagaa
G-olig2	AB038697	5′-ttacagaccgagccaacacc
	U55762	5′-ttgaattcttacttgtacagctcgtcc

PCR primer pairs for *gapdh*, *mbp* intron 1, and the hybrid *Olig2-GFP* locus of Olig2^{GFP}. The primers listed for *mbp* intron 1 represent nested sets, and for G-olig2 the forward primer identifies *Olig2* and the reverse primer corresponds to *GFP* sequences.
Abbreviation: NCBI, National Center for Biotechnology Information; ID, identification.

minutes, then 40 cycles of (95°C for 15 seconds, 55°C for 15 seconds, 72°C for 1 minute). Samples (1 μg genomic DNA) were examined in duplicate using PCR primers (Table 1) that identified wild-type MBP intron 1 and a control gene, glycerol phosphate dehydrogenase (GAPDH). The relative number of Olig2^{GFP}-derived cells in MBP^{shi}:Olig2^{GFP} chimeric animals was determined from the threshold cycle (C_T) for PCR amplification of *mbp* intron 1 and *gapdh*, using the formula $R = 2^{-\Delta\Delta C_T}$ [32]. For each chimera, the C_T ratio (*mbp/gapdh*) was normalized to the C_T ratio of *mbp/gapdh* in wild-type (non-*shi*) animals. All Q-PCR results were compiled after completion of the functional assays, such that the motor function and longevity studies were performed in double-blind format.

Motor Function and Survival

Animals were tested once only on each day, and daily for 2 weeks, commencing at age 2 weeks. Results from the first day of testing (acclimation) were excluded from the analysis. Motor function was determined by placing individual animals, in random order, into a small tray (3 cm in height) containing water (0.5 cm in depth), and recording the time for their complete exit from the tray (supplemental online Movie). The water tray was placed within their home cage during the testing such that the animals reunited with their littermates upon exiting the water tray. The animal cages remained in the same room throughout the testing period to minimize any external influences. For survival analysis, the age of natural death was recorded for individual animals.

Statistical Analyses

Statistical analyses were performed using SAS version 9.1 software (SAS Institute, Cary, NC, http://www.sas.com). One-way analysis of variance and the PROC GLM (general linear model) procedure were used to compare means of motor function performance between MBP^{shi} mice, wild-type mice, and chimeric MBP^{shi}:Olig2^{GFP} mice containing from 0.01%–.1% (group I), 0.1%–5% (group II), or >5% of wild-type (Olig2^{GFP}) cells. Differences with $p < .05$ were regarded as significant. Linear regression was performed with SigmaPlot 8.0 (SPSS Inc., Chicago, http://www.spss.com), using third-order polynomial and confidence intervals set at 99%, to examine the relationship between motor function performance and % wild-type cells.

RESULTS

Shiverer-Olig2^{GFP} Chimerism

The classic model for assessing myelination by exogenous grafts is the dysmyelinating shiverer (MBP^{shi}) mutant mouse [17, 18] with a genomic deletion [33] that spans the *mbp* gene (Fig. 1A). Homozygous shiverer mutants form uncompacted myelin that degenerates. The loss of axonal insulation causes a pronounced movement-stimulated tremor and motor impairment, first visible at 12 days of age, with tonic seizures, late

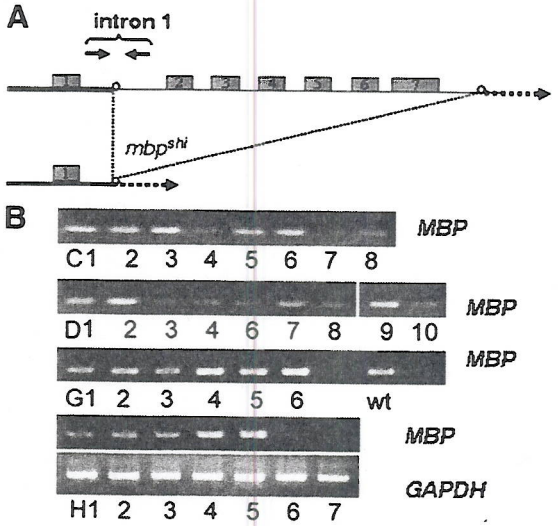

Figure 1. Myelin basic protein (MBP) genomic analysis. **(A):** The *mbp^{shi}* deletion. Polymerase chain reaction (PCR) primers (arrows) spanning the intron 1 deletion breakpoint were used to quantitate Olig2^{GFP}-derived wild-type cells in chimeric animals. **(B):** PCR products for *mbp* and *gapdh* in individual chimeric animals (C1-H7) and wild-type (wt) controls.

onset paralysis, and a shortened life span. However, shiverer nulls are both viable and fertile. The grafting of either OLs or their immediate progenitor cells (OPCs) into neonatal shiverer hosts [34, 35] restores compact myelin [36] and can restore partial function [37].

Our objective was to generate a cohort of MBP^{shi}:Olig2^{GFP} chimeras, with individual animals harboring a range (low to high) of ESC-derived MBP^{wt} cells. We reasoned that the most expedient approach was to generate blastocyst chimeras, where the numbers of grafted cells that participate in organogenesis would be stochastic among recipients, whereas the contribution of ES^{wt} to the three germ layers would be relatively constant within individual chimeras. We grafted ≈14 Olig2^{GFP} ESCs into day-3.5 *shi/shi* blastocysts, and then transferred these to pseudopregnant foster mothers. Chimeric embryos were harvested at days 13.5–15.5 for histochemical studies, and we examined chimeric animals from full-term litters for motor function and life span. There were no significant differences in the number of viable offspring in MBP^{shi}:Olig2^{GFP} chimeric litters at either embryonic days 13, 14, or 15 (31 embryos in three litters) or at full term (29 pups in four litters), and both were equivalent to the litter size of uninjected MBP^{shi} control litters. Thus the grafted Olig2^{GFP} ESCs did not appear to impact early development, consistent with an exclusively postnatal phenotype for the *Mbp^{shi}* allele [38].

Table 2. MBP^{shi}:$Olig2^{GFP}$ chimerism, water avoidance

	C_T (GAPDH)	C_T (MBP)	% wild-type	Time (seconds)
MBP^{wt}	25.07 ± 0.78	22.21 ± 0.72	100	5.47 ± 0.59
MBP^{shi}	25.58 ± 1.64	n.d.	0.00	20.1 ± 1.17
MBP^{shi}:$Olig2^{GFP}$				
F5	22.10 ± 0.23	31.83 ± 0.99	0.02%	19.58 ± 4.58
G7	22.79 ± 0.17	32.5 ± 1.15	0.02%	9.58 ± 2.24
G8	24.21 ± 0.85	32.54 ± 0.83	0.04%	16.03 ± 5.29
G5	23.94 ± 0.32	32.2 ± 1.82	0.04%	21.35 ± 4.31
F7	23.94 ± 0.48	32.1	0.05%	14.48 ± 2.68
F9	25.79 ± 0.25	32.89	0.10%	23.72 ± 5.22
G2	24.51 ± 0.19	31.33	0.12%	22.78 ± 3.42
F6	24.60 ± 0.45	31.14 ± 2.63	0.15%	22.29 ± 5.26
F8	23.15 ± 0.35	29.48 ± 0.57	0.17%	16.17 ± 2.41
G4	24.61 ± 0.34	30.83 ± 0.56	0.18%	10.85 ± 2.10
G3	25.47 ± 0.29	29.66 ± 0.67	0.75%	15.09 ± 2.58
F4	22.24 ± 0.45	26.16 ± 0.17	0.91%	14.12 ± 2.13
H6	22.15 ± 0.38	23.04 ± 0.65	1.62%	13.83 ± 2.71
F2	21.76 ± 0.19	24.11 ± 0.15	2.69%	11.48 ± 2.64
H3	22.55 ± 0.26	23.6 ± 1.05	6.63%	17.97 ± 3.40
G6	24.42 ± 0.73	24.92 ± 0.58	7.25%	5.79 ± 1.35
H2	24.67 ± 0.32	24.65 ± 0.97	13.91%	20.46 ± 3.29
H4	25.08 ± 0.63	24.96 ± 2.24	14.99%	17.05 ± 2.73
H1	24.34 ± 1.32	24.2 ± 2.16	15.16%	15.57 ± 3.02
H7	23.59 ± 0.59	23.24 ± 2.54	17.53%	14.21 ± 2.64
H5	22.99 ± 1.05	22.07 ± 0.80	26.00%	5.27 ± 1.31
G1	22.87 ± 0.34	21.95 ± 1.13	26.05%	5.09 ± 1.28

Quantitative polymerase chain reaction analysis of MBP^{wt} (n = 8), MBP^{shi} (n = 11), and individual MBP^{shi}:$Olig2^{GFP}$ chimeric mice, listed by level of MBP^{wt} chimerism. C_T indicates threshold cycle (mean ± SD) from n = 2–5 independent replicates. Chimerism (% wild-type) was determined by comparing C_T of *mbp* (normalized to *gapdh*) for chimeric animals with normalized *mbp* in wild-type animals (100%). Exit times (mean ± SD) from a water basin were recorded once daily for 2 weeks.
Abbreviations: GAPDH, glycerol phosphate dehydrogenase; MBP, myelin basic protein; n.d., not determined.

To determine the extent of chimerism we used genomic DNA analysis, focusing on Q-PCR amplification of a chromosomal fragment that is unique to wild-type *mbp* intron 1 (Fig. 1A). Attempts to PCR amplify the chromosomal fragment spanning the MBP^{shi} deletion breakpoint were uninformative, possibly due to reiterated sequences downstream of exon 7 that appear to be responsible for the *shi* chromosomal deletion [33]. The Mbp^{wt} intron 1 PCR fragment was absent in *shi/shi* controls and present in most chimeric animals examined, with a broad range of signal strength in individual chimeras (Fig. 1B). To determine the relative level of ESC-derived Mbp^{wt} in each animal, we normalized the threshold (C_T) MBP^{wt} signal to that of a control PCR product (*gapdh*), which is present at the same copy number in both MBP^{shi} (host) and $Olig2^{GFP}$ (graft) cells. The normalized *mbp* levels were then compared with normalized C_T (*mbp/gapdh*) in wild-type (non-*shi*) animals (Table 2). This analysis revealed a range of chimerism from undetectable through 26% $Olig2^{GFP}$. We did not detect any obvious bias for ESC contribution to distinct germ layers in individual chimeras. Relative to brain (1.00), the levels of $Olig2^{GFP}$-derived cells were comparable in heart (1.02), kidney (.87), liver (.62), skeletal muscle (.70), and tail (.99). Importantly, the genomic analysis was performed subsequent to the functional studies described below, and all Q-PCR results were complied post hoc so that the functional outcome was performed in double-blind format.

Shi-$Olig2^{GFP}$ Chimeras Express MBP

To determine whether the ESCs used ($Olig2^{GFP}$) could generate MBP^+ oligodendrocytes we examined both transcript and protein expression (Fig. 2). For in vitro differentiation the cells were first aggregated into embryoid bodies then sequentially exposed to neural induction factors (RA, FGF, Shh) followed by glial cell mitogens (FGF, PDGF) as detailed in Materials and Methods. This process generated cells with the characteristic morphology and marker profile of lineage-committed OPCs and OLs (Fig. 2A), and these were indistinguishable from bona fide OL lineage cells isolated from the neonatal rodent brain [39]. Thus the G-olig2 cells were competent to generate OL lineage cells in vitro.

To determine whether ES^{wt}-derived cells had undergone OL differentiation in vivo, we examined the expression of MBP transcripts (Fig. 2B) and protein (Fig. 2C–2E) in MBP^{shi}:$Olig2^{GFP}$ chimeras. Using RT-PCR, MBP transcripts were observed in most chimeras examined (Fig. 2B, center panels), including both embryonic day 14 (lanes 14a-d) and day 15 (lanes 15a-d). The predominant MBP transcripts were splice variants lacking exon 2, and for several animals we also observed a smaller, earlier emerging transcript lacking exons 2 and 6 (Fig. 2B, lanes 14a, 15a). No MBP transcripts were detected in nongrafted shiverer control animals. OL lineage differentiation of graft-derived cells was also confirmed by expression of hybrid Olig2-GFP transcripts (Fig. 2B, top panels). $Olig2^{GFP}$ cells have the *gfp* transgene inserted within the *olig2* locus, with GFP expression controlled by the endogenous *olig2* cis-regulatory elements [28]. Thus the onset of GFP expression marks the activation of endogenous Olig2, an early marker for OPC fate induction [40]. Consistent with this, hybrid Olig2-GFP transcripts were detected in chimeras that expressed early isoforms of MBP, lacking both exons 2 and 6 (Fig. 2B, lanes 14a, 15a).

Using histochemistry we also detected MBP^+ OLs in whole mount spinal cord preparations of embryonic MBP^{shi}:$Olig2^{GFP}$ chimeras (Fig. 2C–2E). MBP staining was completely absent from shiverer controls. In a single chimera we detected an

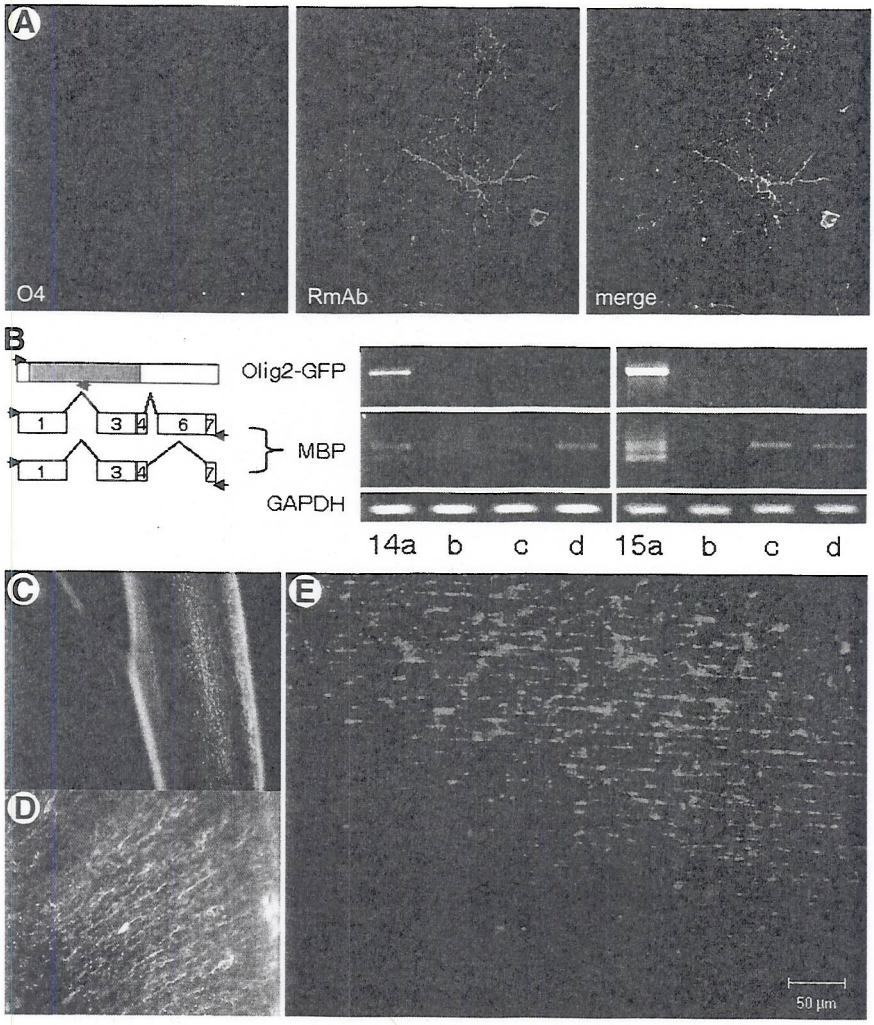

Figure 2. Olig2^{GFP}-derived oligodendrocytes (OLs), in vitro and in vivo. **(A):** OLs in vitro. **(B):** Reverse-transcription–polymerase chain reaction analysis of embryonic day 14 (e14)-e15 spinal cords; primers are shown as arrows on exon maps (left). **(C):** Myelin basic protein-positive (MBP$^+$) OLs in e15 chimera spinal cord; ventral midline is center. **(D):** Dorsal horn of the same cord. **(E):** Olig2^{GFP}-derived myelin sheaths attached to OL soma. Abbreviation: GAPDH, glycerol phosphate dehydrogenase.

asymmetric (mosaic) distribution of MBP in the rostral spinal cord (Fig. 2C). MBP$^+$ OLs were absent from the left and present on the right side of this cord (Fig. 2C). Thus at least some regions of the chimeric neural tube could be generated exclusively from host-derived (MBP^{shi}) cells. This likely represents a stochastic partitioning of grafted ESCs within this neural tube, since our genomic analysis did not identify a bias in contribution of grafted cells to different germ layers. Together with the transcript analysis above, these studies demonstrate that the grafted Olig2^{GFP} ESCs were competent to generate MBP$^+$ OLs in MBP^{shi}:Olig2^{GFP} chimeric animals.

Motor Function Analysis

The shiverer motor tremor first appears at postnatal days 10–12, at the peak of brain myelination, and there are many functional tests that can identify the differences between wild-type and shiverer mice. To address whether Olig2^{GFP} ESC grafts affected the *shi* phenotype, and to quantify any such effects, we developed a sensitive water avoidance assay for motor function (Fig. 3). Beginning at 2 weeks of age, and daily for 2 weeks, animals were placed in a shallow water tray within their home cage and the time required for exit was recorded (supplemental online movie). Wild-type mice had no difficulty in this test, with an exit speed of 5.5 ± 0.6 seconds (Fig. 3A; Table 2). *Shi* control mice, in contrast, had poor motor coordination, difficulty balancing on the tray edge, and an overall slow exit time from this hostile environment (time [t] = 20.1 ± 1.1 seconds; 92 events). There was no obvious deterioration in their motor function over the trial period (Fig. 3B, solid symbols).

In the MBP^{shi}:Olig2^{GFP} chimera cohort, all animals displayed a range of performance ability in the motor function test. Animals were tested in random order on each test day, and subsequent decoding of the results revealed three groups of motor function performance. Of note, all three groups had poor motor performance on the first 3 days of testing. Group I mice (Fig. 3B, open symbols) performed essentially identically (t = 20.1 ± 2.5 seconds; 44 events) to the nongrafted *Shi* controls (p = .94) throughout the testing period. A second group (II) showed an overall 21.6% faster exit time (t = 15.7 ± 1.0 seconds; 69 events; p = .019) relative to *Shi* controls, and the difference with *shi* was most apparent toward the latter test days (Fig. 3C). A third group (III) had a 74.5% faster exit speed (t = 5.7 ± 0.9 seconds; 31 events), significantly faster ($p < .0001$) than the *Shi* controls and essentially equivalent to wild-type (nonshiverer) levels (Fig. 3D). One animal in this group had obvious coat color chimerism and an absence of shiver, whereas all other chimeras retained an obvious tremor and were not readily distinguishable from shiverer controls. Thus the motor function test as used here identified subtle difference in balance and coordination between chimeras and *shi/shi* mutant animals. The consistency of motor performance for animals in each group during the testing period suggests this analysis was an effective metric for the Olig2^{GFP} engraftment levels in these chimeras.

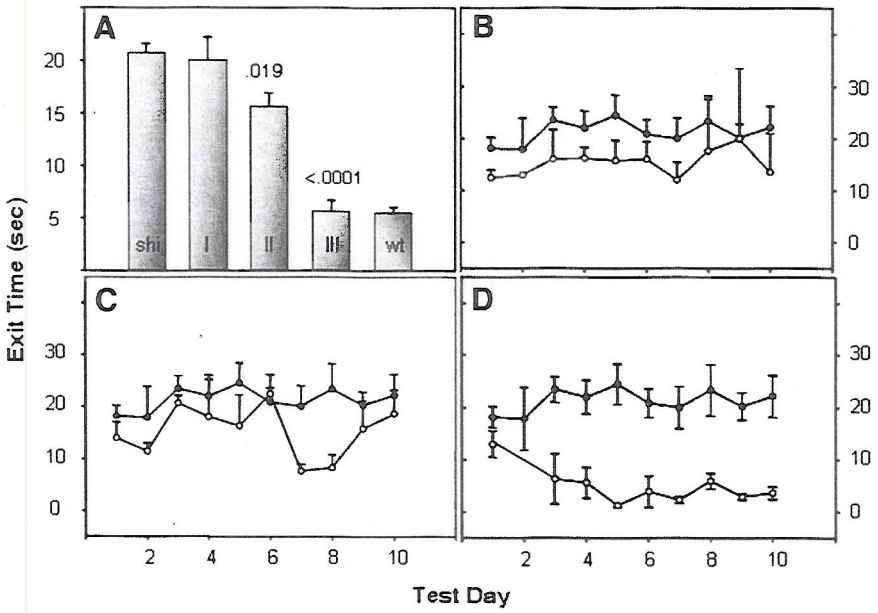

Figure 3. Motor function analysis. **(A):** Exit times for *Mbp*^{shi} mutants, wild-type, and MBP^{shi}:Olig2^{GFP} chimeras. **(B–D):** Daily performance of *Mbp*^{shi} mutants (solid symbols) and MBP^{shi}:Olig2^{GFP} chimeras (open symbols), including **(B)** group I, **(C)** group II, and **(D)** group III chimeras. Group II and III chimeras were significantly faster ($p < .02$) than *Mbp*^{shi}, whereas group I chimeras were not ($p = .94$). Motor function was scored in double-blind format with genotype analysis decoded post hoc. Abbreviation: sec, seconds.

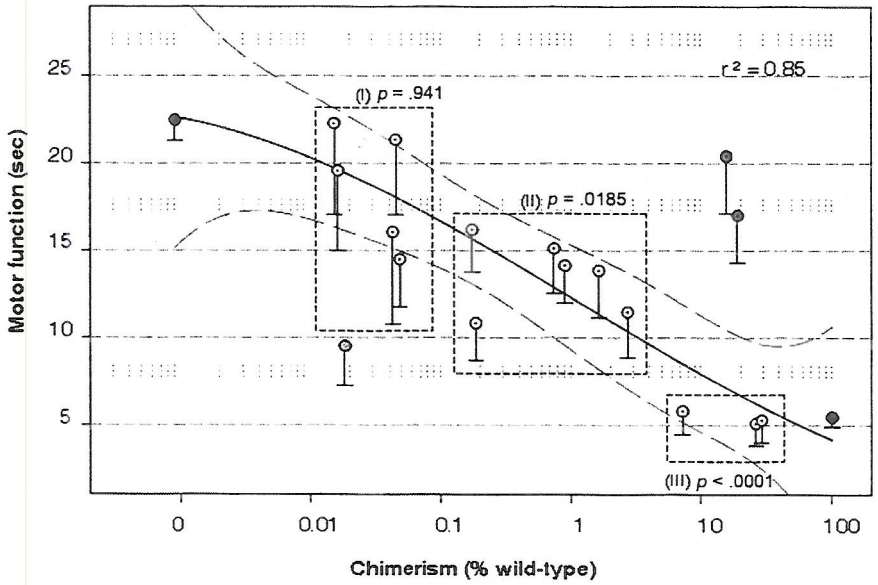

Figure 4. Relationship between chimerism and motor function. Chimerism was determined by threshold cycle using quantitative polymerase chain reaction analysis of genomic DNA, with *mbp* levels normalized to *gapdh* then compared with normalized *mbp* in wild-type animals. Nongrafted controls include *mbp*-null Shiverer (red) and wild-type mice (black symbol). Motor function was as outlined in Figure 3. Abbreviation: sec, seconds.

MBP Chimerism and Motor Function

We next decoded the genomic chimerism data, the results of which identified a strong and surprising relationship ($r^2 = 0.85$) of MBP^{wt} levels to motor performance (Fig. 4). Group I chimeras, which were not significantly faster than age-matched Shi mutants, had less than 0.1% of wild-type cells. Group II chimeras with 22% faster exit speed contained between 0.1%–5% wild-type cells. Group III chimeras, with 75% faster exit speed, contained greater than 7% wild-type cells (Fig. 4). Thus 85% of the variability in motor function can be explained by the level of wild-type cells in these chimeras. Two groups of outliers were excluded in this analysis. One animal showed relatively fast avoidance time (t = 10 seconds) with a low level of detectable chimerism, whereas two animals with higher levels of chimerism performed poorly in the functional assay (Fig. 4). These animals were also outliers based on longevity analysis, as outlined below. Since the results of this study were decoded after the longevity analysis, we were unable to determine whether these outliers represent either germ layer or CNS region-specific mosaic distribution of Olig2^{GFP} grafted cells.

MBP Chimerism and Longevity

Finally we addressed the effect of chimerism on longevity. Age of death was recorded for each animal and the survival curves were tabulated for each of the three groups of cohorts (Fig. 5). Their mortality is thought to be due to anoxia associated with tonic seizures [38]. Shi mutants and chimeras with lower levels of wild-type cells (groups I, II) had a relatively short natural life span with 50% mortality (T_{50}) of 108 days (Fig. 5). In sharp contrast, group III chimeras with greater than 7% wild-type ESCs had a considerably extended life span ($T_{50} > 128$ days). This rather striking relationship was revealed only after the death of all but one animal (H5), who has remained viable as of 620 days. Backcrossing this female to a MBP^{shi} male generated one litter, and all F_1 offspring were homozygous *shi/shi*, consistent with the finding that the parental ESCs are not germ-line competent [28].

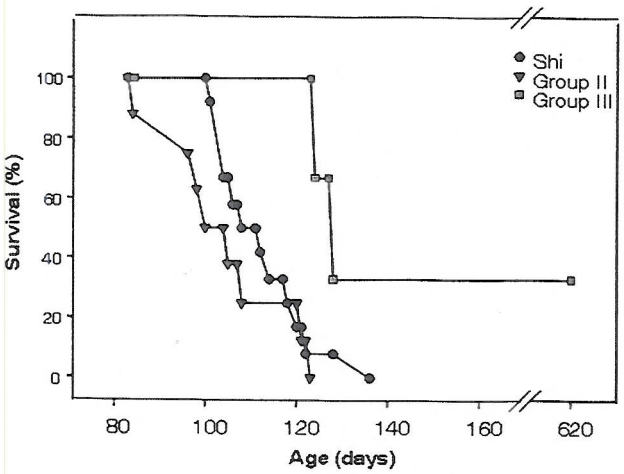

Figure 5. Survival of MBP^{shi}:$Olig2^{GFP}$ chimeras. Age of natural death for MBP^{shi} (circles) and for MBP^{shi}:$Olig2^{GFP}$ chimeras from groups II (triangles) and III (square symbols). Group III chimeras with >20% extended life span relative to MBP^{shi} controls retained a mild tremor.

DISCUSSION

One limitation to evaluating the outcome of cell transplantations has been defining the minimal graft level required for tissue repair and therapeutic recovery. Indeed, the efficiency of cell engraftment has not been addressed in most cell transplant models to date. Here we used quantitative genomic analysis to measure chimerism, and we identify a strong relationship between levels of engraftment and functional benefits of ESC-derived CNS myelin replenishment therapy. At 1% wild-type engraftment there is a small but significant increase in motor function, and above 7% engraftment there are substantial improvements in both motor function and longevity. These results thus establish the minimal levels of graft replacement for therapeutic outcome in a cell-autonomous deficit.

The experimental model we have used, dysmyelinating shiverer mice, has several advantages for this type of analysis. First, the pathology of shiverer mice is limited to the CNS and is distributed throughout the brain and spinal cord. The shiverer animals described in this study were maintained on a common genetic background, and there is no detectable phenotype variation between individual *shi/shi* animals. Second, grafting cells into day-3.5 blastocysts allowed us to deliver a standard number of donor cells to each chimera. The ESC donor cells were expanded under standard culture conditions, and transplantations were performed using a reproducible approach, minimizing any potential variations in both host and graft cell populations. Thus variations in phenotype of the resultant chimeras are a consequence of differences in the numbers of grafted cells that contribute to organogenesis.

One underlying assumption in this study is that individual chimeras with different levels of $Olig2^{GFP}$ engraftment have an equal distribution of graft-derived cells throughout their CNS. The strong relationship observed between motor function and level of engraftment (Fig. 4) lends credibility to this assumption. However this does not eliminate all concerns, and we did find one example of asymmetry in the distribution of MBP-positive cells in the spinal column (Fig. 2C). It is attractive to speculate that a mosaic disequilibrium in graft distribution underlies the three animals who did not fit into our regression analysis (Fig. 4). Whether these outliers reflect an uneven graft distribution requires a detailed analysis that we were not able to address in the present study.

Another question that remains unresolved is what level of compact myelin restoration is necessary for functional rescue. MS patients have a range of symptoms from subtle such as temperature sensitivity to extreme including motor impairment. It is conceivable that lower levels of engraftment and compact myelin restoration could be sufficient, or higher levels necessary, for repair of distinct deficits. Here we focused on general motor function in the shiverer model. The motor function test was by design a simple task to measure coordination, and the consistency of our test results over multiple sample days (Fig. 3) suggests relatively few variables. However, mutant animals did on occasion stop trying to exit, apparently due to fatigue, and it was necessary to omit these data points from our analysis. We have not examined other functional outputs such as balance [37], or more subtle measurements such as axon conduction velocity. In shiverer the myelin deficit affects the entire CNS, whereas demyelinated regions in MS or spinal cord injury involve localized regions or plaques. It is of note that the size of a typical MS plaque can be very large, and the levels of cell replacement required to repair such lesions would likely parallel the order of magnitude required to repair the shiverer brain.

CONCLUSION

The current focus of MS therapy is immune suppression [41]. This is not a cure, and its efficacy remains controversial [42]. There is a need for new therapeutic strategies, and the use of cell transplantations is supported by preclinical studies [4]. However, for clinical transplantations to be effective, they must meet significant hurdles, including avoiding the sensitized immune environment of the MS patient. Thus allografts would require sustained immune suppression and may do more harm than good. In contrast, autologous grafts of either adult stem cells or reprogrammed somatic cells [13, 43] as an emerging field represents a potential and promising alternative. To realize this potential, it will be necessary to address other hurdles, such as targeting the migration of grafted cells toward lesions [4]. Our present results suggest that evaluating the efficacy of alternative graft sources, or the homing of grafted cells into demyelinated lesions, should be evaluated on the criteria of a minimum of 7% replacement for functional improvement.

ACKNOWLEDGMENTS

We thank Drs. Mantu Bhaumik (Transgenic and Knockout Mouse Shared Resources) and Jack Spychala (DNA Core Facilities) for their support, and Drs. Viktor Dombrovskiy (RWJMS-Surgery) and Weichung Joe Shih (School of Public Health and the Cancer Institute of New Jersey) for statistical analysis. This work was supported by grants from the New Jersey Commission on Spinal Cord (05-3047-SCR-E-0) and Stem Cell (06-2042-014-74) Research, and U.S. Public Health Service Grant MH54652 from the National Institute of Mental Health.

DISCLOSURE OF POTENTIAL CONFLICTS OF INTEREST

The authors indicate no potential conflicts of interest.

REFERENCES

1 Lindvall O, Kokaia Z. Stem cells for the treatment of neurological disorders. Nature 2006;441:1094–1096.
2 Björklund A, Dunnett SB, Brundin P et al. Neural transplantation for the treatment of Parkinson's disease. Lancet Neurol 2003;2:437–445.
3 Frohman EM, Racke MK, Raine CS. Medical progress: Multiple sclerosis–The plaque and its pathogenesis. N Engl J Med 2006;354:942–955.
4 Chen CP, Kiel ME, Sadowski D, McKinnon RD. From stem cells to oligodendrocytes: Prospects for brain therapy. Stem Cell Reviews 2007; 3:280–288.
5 Reynolds RA, Weiss S. Generation of neurons and astrocytes from isolated cells of the adult mammalian central nervous system. Science 1992;255:1707–1710.
6 Davis AA, Temple S. A self-renewing multipotential stem-cell in embryonic rat cerebral-cortex. Nature 1994;372:263–266.
7 Morshead CM, Reynolds BA, Craig CG et al. Neural stem cells in the adult mammalian forebrain: a relatively quiescent subpopulation of subependymal cells. Neuron 1994;13:1071–1082.
8 Uchida N, Buck DW, He DP et al. Direct isolation of human central nervous system stem cells. Proc Natl Acad Sci U S A 2000;97: 14720–14725.
9 Evans MJ, Kaufman MH. Establishment in culture of pluripotential cells from mouse embryos. Nature 1981;292:154–156.
10 Martin GR. Isolation of a pluripotent cell line from early mouse embryos cultured in medium conditioned by teratocarcinoma stem cells. Proc Natl Acad Sci U S A 1981:78;7634–7638.
11 Bradley A, Evans M, Kaufman MH, Robertson E. Formation of germline chimeras from embryo-derived teratocarcinoma cell-lines. Nature 1984;309:255–256.
12 Thomson JA, Itskovitz-Eldor J, Shapiro SS et al. Embryonic stem cell lines derived from human blastocysts. Science 1998;282:1145–1147.
13 Takahashi K, Yamanaka S. Induction of pluripotent stem cells from mouse embryonic and adult fibroblast cultures by defined factors. Cell 2006;126:663–676.
14 Wernig M, Meissner A, Foreman R et al. In vitro reprogramming of fibroblasts into a pluripotent ES-cell-like state. Nature 2007;448: 318–324.
15 Okita K, Ichisaka T, Yamanaka S. Generation of germline-competent induced pluripotent stem cells. Nature 2007;448:313–317.
16 Freed CR, Breeze RE, Greene P et al. Transplanted dopaminergic neurons: More or less? Reply [letter]. Nat Med 2001;7:512–513.
17 Bird TD, Farrell DF, Sumi SM. Genetic developmental myelin defect in shiverer mouse. Trans Am Soc Neurochem 1977;8:153.
18 Jacque C, Privat A, Dupouey P et al. Shiverer mouse: A dysmyelinating mutant with absence of major dense line and basic protein in myelin. Proc Eur Soc Neurochem 1978;1:131.
19 Pfeiffer SE, Warrington AE, Bansal R. The oligodendrocyte and its many cellular processes. Trends Cell Biol 1993;3:191–197.
20 Brüstle O, Jones KN, Learish RD et al. Embryonic stem cell-derived glial precursors: A source of myelinating transplants. Science 1999; 285:754–756.
21 Perez-Bouza A, Glaser T, Brustle O. ES cell-derived glial precursors contribute to remyelination in acutely demyelinated spinal cord lesions. Brain Pathol 2005;15:208–216.
22 Keirstead HS, Nistor G, Bernal G et al. Human embryonic stem cell-derived oligodendrocyte progenitor cell transplants remyelinate and restore locomotion after spinal cord injury. J Neurosci 2005;25: 4694–4705.
23 Izrael M, Zhang PL, Kaufman R et al. Human oligodendrocytes derived from embryonic stem cells: Effect of noggin on phenotypic differentiation in vitro and on myelination in vivo. Mol Cell Neurosci 2007;34: 310–323.
24 Groves AK, Barnett SC, Franklin RJM et al. Repair of demyelinated lesions by transplantation of purified O-2A progenitor cells. Nature 1993;362:453–455.
25 Warrington AE, Barbarese E, Pfeiffer SE. Stage specific, (O4+GalC-) isolated oligodendrocyte progenitors produce MBP+ myelin in vivo. Dev Neurosci 1992;14:93–97.
26 Tontsch U, Archer DR, Dubois-Dalcq M, Duncan ID. Transplantation of an oligodendrocyte cell line leading to extensive myelination. Proc Natl Acad Sci U S A 1994;91:11616–11620.
27 Readhead C, Popko B, Takahashi N et al. Expression of a myelin basic protein gene in transgenic shiverer mice: Correction of the dysmyelinating phenotype. Cell 1987;48:703–712.
28 Xian HQ, McNichols E, St Clair A, Gottlieb DI. A subset of ES-cell-derived neural cells marked by gene targeting. Stem Cells 2003;21: 41–49.
29 Billon N, Jolicoeur C, Ying QL et al. Normal timing of oligodendrocyte development from genetically engineered, lineage-selectable mouse ES cells. J Cell Sci 2002;115:3657–3665.
30 Sommer I, Schachner M. Monoclonal antibodies (01 to 04) to oligodendrocyte cell surfaces: An immunocytological study in the central nervous. Dev Biol 1981;83:311–327.
31 Ranscht B, Clapshaw PA, Price J et al. Development of oligodendrocytes and Schwann cells studied with a monoclonal antibody against galactocerebroside. Proc Natl Acad Sci U S A 1982;79:2709–2713.
32 Livak KJ, Schmittgen TD. Analysis of relative gene expression data using real-time quantitative PCR and the 2(T)(-Δ Δ C) method. Methods 2001;25:402–408.
33 Molineaux SM, Engh H, De Ferra F et al. Recombination within the myelin basic protein gene created the dysmyeinating shiverer mouse mutation. Proc Natl Acad Sci U S A 1986;83:7542–7546.
34 Gumpel M, Baumann N, Raoul M, Jacque C. Survival and differentiation of oligodendrocytes from neural tissue transplanted into new-born mouse brain. Neurosci Lett 1983;37:307–311.
35 Lachapelle F, Gumpel M, Baulac M et al. Transplantation of CNS fragments into the brain of shiverer mutant mice: Extensive myelination by implanted oligodendrocytes. I. Immunohistochemical Studies. Dev Neurosci 1983;6:325–334.
36 Gansmuller A, Lachapelle F, Baron-Van Evercooren A et al. Transplantation of newborn CNS fragments into the brain of shiverer mutant mice: Extensive myelination by transplanted oligodendrocytes. II. Electron microscopic study. Dev Neurosci 1986;8:197–207.
37 Kuhn PL, Petroulakais E, Zazanis GA, McKinnon RD. Motor function analysis of myelin mutant mice using a rotarod. Int J Dev Neurosci 1995;13:715–722.
38 Chernoff GF. Shiverer: An autosomal recessive mutant mouse with myelin deficiency. J Hered 1981;72:128.
39 McKinnon RD, Smith C, Behar T et al. Distinct effects of bFGF and PDGF on oligodendrocyte progenitor cells. Glia 1993;7:245–254.
40 Lu QR, Sun T, Zhu Z et al. Common developmental requirement for olig function indicates a motor neuron/oligodendrocyte connection. Cell 2002;109:75–86.
41 Vogel F, Hemmer B. New immunomodulatory treatment strategies in multiple sclerosis. Nervenheilkunde 2002;21:508–511.
42 Marrie RA, Rudick RA. Drug Insight: Interferon treatment in multiple sclerosis. Nat Clin Pract Neurol 2006;2:34–44.
43 Wakayama T, Tabar V, Rodriguez I et al. Differentiation of embryonic stem cell lines generated from adult somatic cells by nuclear transfer. Science 2001;292:740–743.


See www.StemCells.com for supplemental material available online.